July 2004, Vol.19, No.4, pp.529-537 J. Comput. Sci. & Technol.

Realistic Modeling and Animation of Human Body Based on Scanned Data

Yong-You Ma[1,2], Hui Zhang[2], and Shou-Wei Jiang[2]

[1] *School of Mechanical Engineering, East China University of Science and Technology Shanghai 200237, P.R. China*

[2] *School of Mechanical Engineering, Shanghai Jiaotong University, Shanghai 200030, P.R. China*

E-mail: yongyouma@sina.com

Received April 7, 2003; revised September 17, 2003.

Abstract In this paper we propose a novel method for building animation model of real human body from surface scanned data. The human model is represented by a triangular mesh and described as a layered geometric model. The model consists of two layers: the control skeleton generating body animation from motion capture data, and the simplified surface model providing an efficient representation of the skin surface shape. The skeleton is generated automatically from surface scanned data using the feature extraction, and then a point-to-line mapping is used to map the surface model onto the underlying skeleton. The resulting model enables real-time and smooth animation by manipulation of the skeleton while maintaining the surface detail. Compared with earlier approach, the principal advantages of our approach are the automated generation of body control skeletons from the scanned data for real-time animation, and the automatic mapping and animation of the captured human surface shape. The human model constructed in this work can be used for applications of ergonomic design, garment CAD, real-time simulating humans in virtual reality environment and so on.

Keywords human body modeling, 3D reconstruction, animation, real-time, deformation

1 Introduction

Creating virtual human body with physical realism is one of the most demanding tasks in the fields of human modeling and animation. Such models are of increasing importance in a number of application areas, in particular, ergonomic design, clothing industry, medical research and virtual reality. However, convincingly modeling human shape, appearance and motion is very difficult.

In general, surface is the most expressive and important section in geometric modeling of human body. In recent years, high quality 3D models of real human body can be obtained from some commercial systems[1], based on the surface measurement techniques, such as laser scanning and stereo photogrammetry. Nowadays high resolution scanners are capable of acquiring 100,000 to 500,000 coordinate data points for shape measurement. Surface reconstruction results in an unstructured polygonal mesh representation of the surface. This is a highly inefficient representation, as smooth surface is modeled at the same resolution as smooth detail regions. A number of mesh optimization algorithms have been proposed to process the redundant meshes obtained from surface reconstruction[2-4]. The objective of these algorithms is to automatically reduce the number of polygons while maintaining an accurate and realistic representation. Wang *et al.*[5] presented a feature-based mesh generation algorithm to construct the mesh surface of a human model from a point cloud. The whole system is based on fuzzy logic concept. Although they are sufficient for static human model, the surface data contain no structure for animation.

Realistic animation of 3D human body model typically involves two main aspects: realistic motion and smooth deformation of the body. Models used in the majority of motion control researches are skeleton based[6]. A variety of approaches have been proposed for deformable animation of articulated bodies, such as metaballs[7], free-form deformations (FFD)[8], implicit surfaces, hierarchical B-splines[9], physics-based deformable models[10] and pose space deformation[6]. It must be pointed out that all of these techniques aim at creating and animating synthetic computer-generated characters. None of these attempts have produced a highly realistic body shape for a specific person. The issue of efficient and realistic deformation of a polygo-

*Correspondence

This work is supported by the National Natural Science Foundation of China (Grant No.60174023) and the National Research Foundation for the Doctoral Program of Higher Education of China (Grant No.20010248008).

nal model with an internal skeleton is addressed in many CG and game packages[11]. But users are usually required to enter data at the vertex level to map characters to the bones manually.

Using a layered construction approach to build animated synthetic models has been addressed by many researchers. Sun *et al.*[12] constructed a layered model to animate the scanned human body. Their model consists of three layers: a skeleton, a low resolution control model and a high resolution surface model. Since multilayer maps are concerned, their algorithm is very much time-consuming. Brett *et al.*[13] presented an example-based method for calculating skeleton-driven body deformations. The detailed deformations are represented as displacements from a postural subdivision surface template, and holes are filled smoothly within the displacement maps. However, in their method, the scanned data of human body in a variety of poses have to be supplied. The efficient and realistic animation of captured data is still an open problem.

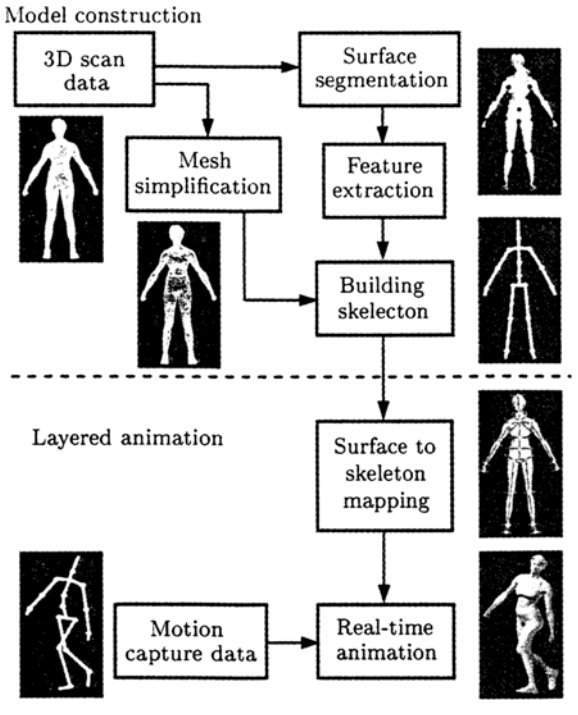

Fig.1. System frame overview.

The goal of our research is to enable reconstruction of the human body model suitable for animation from the scanned data realistically and efficiently. In this paper, the human model is represented by a triangular mesh and described as a layered model. Our model consists of two layers: the skeleton model providing animation from key-frame or motion capture data; and the simplified mesh surface model providing an efficient representation of the skin surface shape and detail. Fig.1 shows an overview of the system. It includes two parts: model construction and layered animation. The surface model is constructed from the high resolution scanned data, which is obtained from a Cyberware laser scanning system[14] and refined by using the techniques of surface reconstruction[15] and mesh simplification[16]. We use fully automatic techniques for segmenting the 3D body scans and locating their key landmarks[17]. These surface landmarks are close to the joint locations where we wish to articulate the model. A robust automatic skeleton generation method is presented by making use of the key landmarks, and then a point-to-line map technique is applied to generating smooth body deformation and real-time animation. Compared with the earlier methods, the advantages of our approach are the automated generation of body control skeletons from the scanned data, and the automatic mapping for real-time animation of the captured human surface shape.

2 Layered Human Model Representation

2.1 Control Skeleton Model

The human body skeleton is formed by 206 bones attached to each other at joints. In our work, we used a simplified model of the human skeleton which contains 19 parts connected by 16 joints (including the multiplex joints, see Fig.2). On account of the complexity, neither facial animation nor hands and feet deformations are considered in this paper. The skeleton model has a hierarchical structure, which can be represented by a tree, where the root is the hip. Each part of the skeleton is regarded as a rigid link, and each joint is assigned to three rotational degrees of freedom (DOF).

We use the three-dimensional coordinate systems shown in Fig.2 to describe the position of body joints. The position of the whole human body is represented by three-dimensional coordinates of the hip relative to the world coordinates system. On each link, a local coordinate system is put to describe the position of the next link sequentially. The origin is set at the joint that connects the link with its previous link. The orientation of each link is described by the three direction angles in the local coordinate system, and the position of each

joint is decided by the length and orientation of its parent link.

The initial posture of the body is set as upstanding. In order to establish the motion relation of links, we describe the position of each link (or joint) with a vector, which is represented under the corresponding local coordinate system (see Fig.2). We assume that the unit base vector of the world coordinate system is expressed as $\boldsymbol{x}_0, \boldsymbol{y}_0, \boldsymbol{z}_0$, so the base vector system can be represented as:

$$[\boldsymbol{a}_0]^{\mathrm{T}} = [\boldsymbol{x}_0\ \boldsymbol{y}_0\ \boldsymbol{z}_0]. \tag{1}$$

Similarly, the base vector of the j-th local coordinate system is represented as:

$$[\boldsymbol{a}_j]^{\mathrm{T}} = [\boldsymbol{x}_j\ \boldsymbol{y}_j\ \boldsymbol{z}_j] \tag{2}$$

where j stands for the index of the local coordinate system in the hierarchical structure starting from the root.

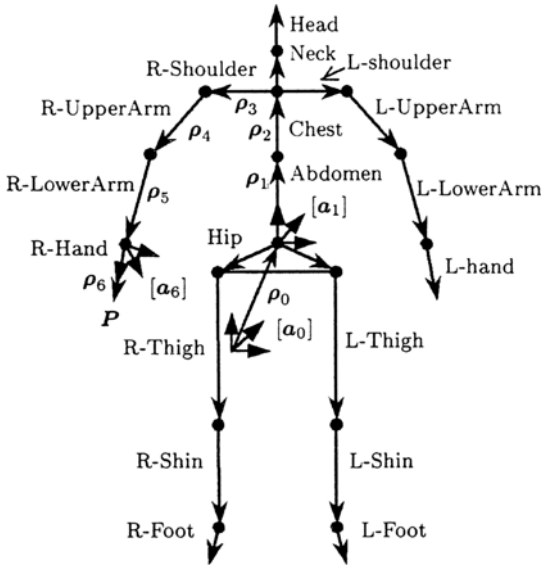

Fig.2. Skeleton structure, position of joints and coordinate systems.

The position of each joint can be calculated by performing a coordinate transformation with Euler angular matrices[18,19]. In this transformation, the local coordinate systems are first rotated around the z axis by angle γ, then around y axis by angle β, and around x axis by angle α. The corresponding rotation matrices around the z, y, x axes are respectively represented as $R_z(\gamma)$, $R_y(\beta)$, $R_x(\alpha)$. The rotation transformation matrix from the coordinate system $[\boldsymbol{a}_j]$ to $[\boldsymbol{a}_{j-1}]$ can be expressed by:

$$\boldsymbol{R}_j = R_x(\alpha_j) \cdot R_y(\beta_j) \cdot R_z(\gamma_j) \tag{3}$$

where

$$\begin{cases} R_x(\alpha_j) = \begin{bmatrix} 1 & 0 & 0 \\ 0 & \cos\alpha_j & -\sin\alpha_j \\ 0 & \sin\alpha_j & \cos\alpha_j \end{bmatrix} \\ R_y(\beta_j) = \begin{bmatrix} \cos\beta_j & 0 & \sin\beta_j \\ 0 & 1 & 0 \\ -\sin\beta_j & 0 & \cos\beta_j \end{bmatrix} \\ R_z(\gamma_j) = \begin{bmatrix} \cos\gamma_j & -\sin\gamma_j & 0 \\ \sin\gamma_j & \cos\gamma_j & 0 \\ 0 & 0 & 1 \end{bmatrix}. \end{cases} \tag{4}$$

The matrix for the transformation from local coordinates to the world coordinates can be obtained with the equation:

$$\boldsymbol{T}_j = \boldsymbol{R}_1 \cdot \boldsymbol{R}_2 \cdots \boldsymbol{R}_j = \prod_{i=1}^{j} \boldsymbol{R}_i \tag{5}$$

For a tip point P of right hand, we use the hierarchical transformation matrices to calculate its position relative to the world coordinate system. The point P is described by a vector $\boldsymbol{\rho}_6$ in the local coordinate system, and a set of parent links is represented respectively as vectors $\boldsymbol{\rho}_5, \boldsymbol{\rho}_4, \ldots, \boldsymbol{\rho}_1$, while the position of hip is expressed by vector $\boldsymbol{\rho}_0$ in the world coordinate system. As a result, the three-dimensional position of the point P in the world coordinate system can be described by the vector $\boldsymbol{p}$, which is calculated by the following equation:

$$\boldsymbol{p} = \boldsymbol{\rho}_0 + \sum_{j=1}^{6} \boldsymbol{T}_j \boldsymbol{\rho}_j. \tag{6}$$

With the method described above, all the postures of the body skeleton can be determined by giving the position of the hip and the Euler angles of each link.

2.2 Feature Extraction and Segmentation

In the surface model construction process, a number of assumptions must be valid for it to work. In general, these assumptions have something to do with the posture of the body. In the anthropometric posture described here, the subject stands with the feet in between 10cm and hip width apart, and arms held slightly away from the body. The aim is to keep a few centimeters between the arm and torso to aid segmentation. Subjects are scanned in a close-fitting underwear to expose the body shape.

The Cyberware body scanner data can be conveniently represented as a set of horizontal data slices made of 3D vertices. In the absence of such a representation one can use octrees to query and convert the object body into equivalent slices. Dekker and Buxton[17] described the feature detection and segmentation process in detail, and we will only briefly review the process here. At a high level, primary landmarks are detected such as the top of the head, torso, neck, left and right armpits, crotch, and the ends of the arms and legs. These first landmarks are detected by algorithms such as that designed to locate the armpits from a reentrant surface condition as illustrated in Fig.3. The centroid of each horizontal data slice is calculated, and the vertices binned into sectors of angular width φ, which is related to the number of samples in the slice. The arms can be segmented from the torso by detecting the transition slice indicating the branching point at the armpits. Sector bins will typically contain only a few vertices, but when the branching at the armpit occurs, a tolerance can be set to detect the increase in a number

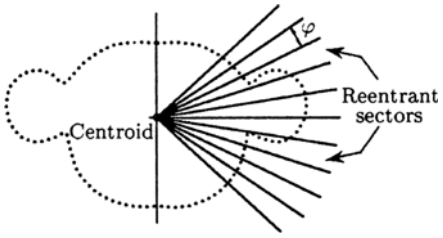

Fig.3. Underarm segmentation using reentrant point tolerance criteria.

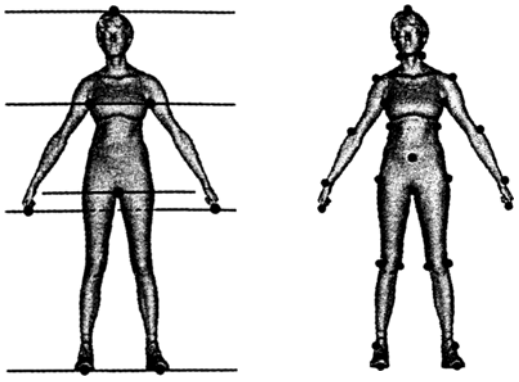

Fig.4. Surface feature extraction. (a) Primary landmarks and sub-search areas. (b) Detected surface landmarks on the human model.

of vertices in a bin. Similarly the neck and crotch can be detected by reasoning about the average distance to the centroid from slice to slice, and about changes in depth[17]. The detected primary landmarks define sub-search areas on the surface of the body scan. In the sub-search areas, a variety of discriminant functions use local shape characteristics like curvature to detect other landmarks, such as shoulder, elbow, wrist, waist, hip, knee and ankle (see Fig.4).

2.3 Mesh Simplification

As the scanned human models are composed of millions of vertices and triangles, applying deformation approach directly to all vertices of the original model is computationally unfeasible for real-time animation rates. To overcome these difficulties, we used the simplification method of Oliveira and Buxton[16]. In particular, since this method uses automatic edge orientation constraints to ensure a global mesh structure suitable for good normal interpolation at lower levels of detail, we should be able to articulate and animate crowd scenes that require high-quality and low-level detailed rendering of humans, for example, by texture mapping facial details and clothing on to our models as in the work of Hilton *et al.*[20]. Fig.5(a) shows the original body scan surface (121,723 vertices, 243,442 triangles), and in Figs.5(b), 5(c), the simplified surface is reduced to about 4% of original data quantity (4,831 vertices, 9,658 triangles), which can be used for real-time animation.

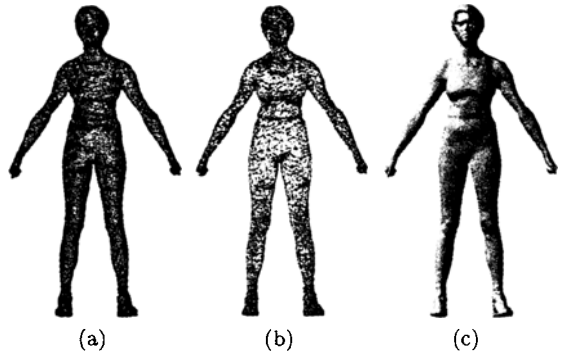

Fig.5. Mesh simplification. (a) Original body scan model of 121,732 vertices, 243,442 triangles. (b) Simplified model of 4,831 vertices, 9,658 triangles (wire frame). (c) Smooth shading model of (b).

In addition, this simplification method yields a robust and clean approximation to the medial axes of the body parts, which can later be used for find-

ing the appropriate joint positions of the skeleton. The medial axes approximation consists of a set of computed centroid vertices from each slice of the high resolution scan (see Fig.6(a)).

2.4 Building Skeleton in Surface Model

We use the detected surface landmarks together with the axes which are regarded as defining an approximate medial axis to find the matching skeleton (Fig.6(a)). The approximate medial axes were generated by joining the centroid of all the horizontal data slices of the model. For each surface landmark (neck, chest, waist, shoulder, elbow, wrist, knee and ankle etc.), we compute the distance to each vertex in the approximate medial axis, and choose the vertex on the approximate medial axis with the shortest distance being the corresponding joint position. Since the model is segmented as described in Subsection 2.2, the search on the approximate medial axis set for the point that represents the joint corresponding to a surface landmark is reduced to a small quantity of calculations.

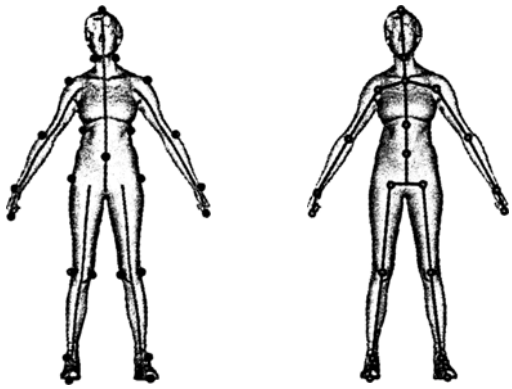

Fig.6. Building the skeleton based on landmarks. (a) Surface landmarks and medial axis approximation. (b) Resulting skeleton segments and joints position.

Considering that real human skeletal joints do not necessarily lie on the medial axis, the automatic skeleton generating method described here has a certain extent error, but then the influence on later animation is slight. Because of the limitation of this automatic method, some joints, such as the upper torso and abdominal joints, are difficult to be detected. To comply with the hierarchy topology of the human anatomy and the skeleton-simplified measure, these joints are determined by making use of the ratios of skeleton segments[21]. Fig.6(b) shows the skeleton generating automatically from the simplified human model of Fig.5, based on the surface key landmarks.

3 Human Model Deformation and Animation

The layered model produced by the aforementioned procedures is realistic and faithful to the personalized original data on the whole. However, it is a static model representing only a certain posture of the human body. In order to deform the body surface properly and obtain the realistic and efficient animation, we had to establish the relationship between the surface model and the skeleton model, and then reconstruct the surface model according to the motion-captured data of rotations and translations from the skeleton structure.

3.1 Mapping of Surface Model to Skeleton

After fitting the skeleton to the surface model, we need to divide the surface mesh layer into several parts based on the skeleton, and then map the points of the surface into their corresponding skeleton segments. The mapping is based on a single posture of the subject. To enable animation of the surface model from the skeleton animation, the mapping of a point to a skeleton segment is parameterized in terms of the joint angles for both ends of the segment. In this paper we make use of a point-to-line mapping which produces full deformation (twist, shear, stretch and compression) of the segment geometry according to the joint angles. This parameterization enables smooth deformation of the mesh for chained joint segments without artifacts such as thinning and sharp edges.

The surface model mapping and animation are based on the concept of *joint planes*. Each joint has an associated joint plane, which equally bisects the angle of the joint and is orthogonal to the plane decided by adjacent joints. The extremities of the skeleton are also considered to be joints for the purposes of this deformation method. Fig.7 illustrates the joint planes for a section of the skeleton. For the i-th skeleton joint with position $\boldsymbol{o}_i$, the i-th joint plane is defined by the local coordinates system based on the positions of adjacent parent and child joints, $\boldsymbol{o}_{i-1}$ and $\boldsymbol{o}_{i+1}$, so that it bisects the joint angle. The local coordinate system $[\boldsymbol{x}_i, \boldsymbol{y}_i, \boldsymbol{z}_i]$ is defined such that the x-axis is normal to the plane defined by the joint positions $(\boldsymbol{o}_{i-1}, \boldsymbol{o}_i, \boldsymbol{o}_{i+1})$; the y-axis is aligned with the joint plane normal;

and the z-axis bisects the angle $\angle \boldsymbol{o}_{i-1}\boldsymbol{o}_i\boldsymbol{o}_{i+1}$. The unit base vector can be represented as:

$$\begin{cases} \boldsymbol{x}_i = \dfrac{(\boldsymbol{o}_{i+1} - \boldsymbol{o}_i) \times (\boldsymbol{o}_i - \boldsymbol{o}_{i-1})}{\|(\boldsymbol{o}_{i+1} - \boldsymbol{o}_i) \times (\boldsymbol{o}_i - \boldsymbol{o}_{i-1})\|} \\ \boldsymbol{z}_i = \dfrac{\boldsymbol{x}_i \times (\boldsymbol{o}_{i+1} - \boldsymbol{o}_i) + (\boldsymbol{o}_{i-1} - \boldsymbol{o}_i) \times \boldsymbol{x}_i}{\|\boldsymbol{x}_i \times (\boldsymbol{o}_{i+1} - \boldsymbol{o}_i) + (\boldsymbol{o}_{i-1} - \boldsymbol{o}_i) \times \boldsymbol{x}_i\|} \\ \boldsymbol{y}_i = \boldsymbol{z}_i \times \boldsymbol{x}_i. \end{cases} \tag{7}$$

It must be noticed that the local coordinate systems defined here are different from those described in Subsection 2.1, which are fixed on the links all the time.

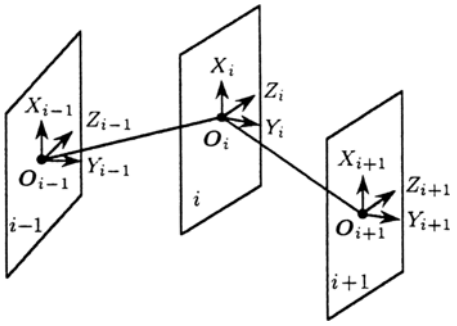

Fig.7. Joint planes and local coordinate systems.

If a joint does not have segments on both sides, as it will occur at the extremities of the skeleton, the joint plane is considered to be orthogonal to the single adjacent segment, with x-axis equal to the parent-joint axis, defined as follows:

$$\boldsymbol{x}_i = \boldsymbol{x}_{i-1}, \quad \boldsymbol{y}_i = \boldsymbol{o}_i - \boldsymbol{o}_{i-1}, \quad \boldsymbol{z}_i = \boldsymbol{x}_i \times \boldsymbol{y}_i.$$

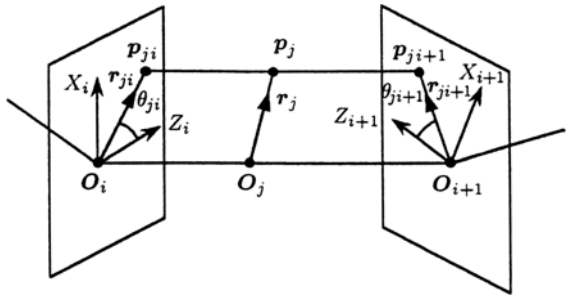

Fig.8. Mapping surface points to a skeleton.

These joint planes move with the skeleton, always bisecting the joint angle whatever joint position and rotation. Each segment will be bounded by at least two joint planes, which allows us to parameterize the vertices affected by that segment in terms of a local coordinate system based upon the joint planes. The problem of calculating which skeleton segment a surface vertex $\boldsymbol{p}_j$ should be mapped to is converted to the problem of determining the two joint planes that the vertex lie in between (see Fig.8). After finding which segment a vertex should be attached to, we want to represent it in local coordinate system with respect to the segment's two joint planes. The point can then be animated according to the movement of the joint planes resulting from skeletal animation.

As illustrated in Fig.8, we project the point $\boldsymbol{p}_j$ parallel to the segment vector $(\boldsymbol{o}_{i+1} - \boldsymbol{o}_i)$ onto each end joint plane, to the project points $\boldsymbol{p}_{ji}$ and $\boldsymbol{p}_{ji+1}$. The normalized vectors $\boldsymbol{r}_{ji} = (\boldsymbol{p}_{ji} - \boldsymbol{o}_i)/\|\boldsymbol{p}_{ji} - \boldsymbol{o}_i\|$ and $\boldsymbol{r}_{ji+1} = (\boldsymbol{p}_{ji+1} - \boldsymbol{o}_{i+1})/\|\boldsymbol{p}_{ji+1} - \boldsymbol{o}_{i+1}\|$ in the joint planes can be expressed in terms of the corresponding joint plane coordinate system as follows:

$$\begin{cases} \boldsymbol{r}_{ji} = \cos(\theta_{ji})\boldsymbol{z}_i + \sin(\theta_{ji})\boldsymbol{x}_i \\ \boldsymbol{r}_{ji+1} = \cos(\theta_{ji+1})\boldsymbol{z}_{i+1} + \sin(\theta_{ji+1})\boldsymbol{x}_{i+1} \end{cases} \tag{8}$$

where θ_{ji} is the angle between $\boldsymbol{r}_{ji}$ and $\boldsymbol{z}_i$. The mapping for vertex $\boldsymbol{p}_j$ to segment $(i, i+1)$ is given by

$$\begin{aligned} \boldsymbol{p}_j = \boldsymbol{o}_j + d_j\boldsymbol{r}_j = \alpha_j\boldsymbol{o}_i + (1-\alpha_j)\boldsymbol{o}_{i+1} + \\ d_j[\alpha_j\boldsymbol{r}_{ji} + (1-\alpha_j)\boldsymbol{r}_{ji+1}] \end{aligned} \tag{9}$$

where $\alpha_j = \|(\boldsymbol{p}_{ji+1} - \boldsymbol{p}_j)\|/\|(\boldsymbol{p}_{ji+1} - \boldsymbol{p}_{ji})\|$, this parameter encodes the distance of point $\boldsymbol{p}_j$ between the bounding joint planes. It can range from 0 to 1, where 0 indicates that the point lies on the plane $i+1$, and 1 indicates that the point lies on the plane i. $\boldsymbol{r}_j$ is given by linear interpolation of vectors $\boldsymbol{r}_{ji}$ and $\boldsymbol{r}_{ji+1}$, d_j is the scale factor along the interpolated vector $\boldsymbol{r}_j$. It should be noted that d_j is not an Euclidean distance, as the interpolated normal does not necessarily have unit length.

This mapping represents a mesh surface point $\boldsymbol{p}_j$ attached to skeleton segment $(i, i+1)$ with four parameters $\alpha_j, d_j, \theta_{ji}, \theta_{ji+1}$. This parameterization forms the basis for animating mesh vertices attached to the segment presented in Subsection 3.2. As the skeleton is animated, the point is the subject to stretch, shear and twist movements.

The surface model is mapped to the skeleton using the point-to-line mapping defined by (9), and for each vertex $\boldsymbol{p}_j$ we can obtain four parameters $(\alpha_j, d_j, \theta_{ji}, \theta_{ji+1})$ from (8) and (9). Each vertex is attached to the nearest segment for which it lies in between the corresponding segment joint planes. For simple skeletal structures, such as the arm and leg, this enables automatic mapping of the surface model to the skeleton. For more complicated structure, such as the shoulder, it is necessary to impose

additional constraints on the point attachments to ensure those points from other parts of the mesh, such as the torso, are not mapped to the arm. Fig.9 shows the result of mapping and surface separation using joint planes. Having defined a mapping for all vertices on the surface mesh to the skeleton, the parameterization enables real-time seamless deformation of the surface model.

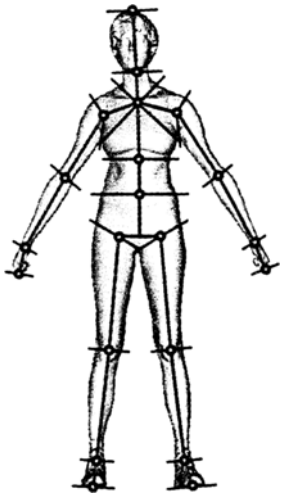

Fig.9. Surface separation using joint planes (additional plane constraints were imposed in some joints).

3.2 Layered Model Animation

The mapping algorithm attaches the surface mesh to the skeleton automatically, but this mapping is performed only for a single posture of the surface model. Geometric mesh deformation[22,23] has previously been used for seamless animation. In this section we use the point-to-line mapping and parameterization presented above to achieve a real-time and smooth deformation of the surface model during animation.

When the skeleton layer is animated, the joints will change the position, both globally and relatively to one another. Therefore, the joint planes will also change. As our parameterization of the mesh vertices between the planes is based on the joint planes, the mesh surface between them is deformed as they move. For each posture of the skeleton during the movement, we first calculate the orientations of new joint planes as discussed in Subsection 3.1. Then for each vertex in the surface model we use the mapping results and joint local coordinates systems in two joint planes to calculate $\boldsymbol{r}'_{ji}$ and $\boldsymbol{r}'_{ji+1}$:

$$\begin{cases} \boldsymbol{r}'_{ji} = \cos(\theta_{ji})\boldsymbol{z}'_i + \sin(\theta_{ji})\boldsymbol{x}'_i \\ \boldsymbol{r}'_{ji+1} = \cos(\theta_{ji+1})\boldsymbol{z}'_{i+1} + \sin(\theta_{ji+1})\boldsymbol{x}'_{i+1} \end{cases} \tag{10}$$

where $\boldsymbol{x}'_i, \boldsymbol{z}'_i, \boldsymbol{x}'_{i+1}, \boldsymbol{z}'_{i+1}$ are the corresponding unit base vectors of changed joint coordinates systems, θ_{ji} and θ_{ji+1} are known from the mapping process. Finally using the parameters α_j and d_j from (9) we have a new vertex position:

$$\boldsymbol{p}'_j = \alpha_j \boldsymbol{o}'_i + (1-\alpha_j)\boldsymbol{o}'_{i+1} + sd_j[\alpha_j \boldsymbol{r}'_{ji} + (1-\alpha_j)\boldsymbol{r}'_{ji+1}] \tag{11}$$

Note that in (11) $\boldsymbol{o}'_i$ and $\boldsymbol{o}'_{i+1}$ are new joint positions, known from joint animation; α_j and d_j are known from the mapping process. The scalar s is introduced to ensure that points maintain a fixed distance d_0 from the nearest point on the skeleton axis. If the nearest point to $\boldsymbol{p}'_j$ on the skeleton axis is outside the joint locations $\boldsymbol{o}'_i$ and $\boldsymbol{o}'_{i+1}$, then the distance d_0 is taken from the nearest joint; otherwise the distance is taken to the nearest point on the axis. This prevents the segment from collapsing under large joint rotations or twists, and eliminates thinning of the mesh along the axis and sharp crease edges near the joints.

The method presented above gives a smooth and continuous deformable animation of the surface model based on the skeleton. As most of the calculations performed for each point are linear interpolations, the reconstruction is highly efficient and can be performed in real time. The anti-thinning calculations require more computations, but the cost is not excessive, considering the improvement in visual quality. The result is a smooth deformation of the mesh surface based on geometric computations which are highly efficient.

4 Results

The presented framework for the construction of layered animation models has been tested on full body data-sets captured by using the Cyberware whole body scanner. The original human surface model has 121,723 vertices and 243,442 triangles. After simplification, the surface data-sets are reduced to 4,831 vertices and 9,658 triangles, as discussed in Subsection 2.3. In our human animation system, we apply motion sequences described by skeleton joint angles to animating the human model. Table 1 gives some examples of motion-captured data of body parts for animation. The results of surface model animation are shown in

Table 1. The Motion Capture Data of Body Parts for Animation

Body parts	Y, X, z Rotation angle of body parts in different posture (deg.)					
	(a)	(b)	(c)	(d)	(e)	(f)
Hip	0, 0, 0	−36, 0, 0	−60, 0, −1	−50, 0, −1	−82, −1, 7	−8, 0, −5
Abdomen	0, 0, 0	0, 0, 0	3, 0, 0	3, 0, 0	−19, 0, −2	3, 0, 0
Chest	0, 0, 0	0, 0, 0	0, 1, 3	0, 3, 5	−11, 1, −2	0, 3, 5
Neck	0, 0, 0	0, 0, 0	0, 1, 1	0, 1, 1	22, 0, 0	0, 1, 1
Head	0, 0, 0	0, −1, 5	0, −1, −1	0, −4, −5	18, 2, 4	0, −1, −1
Left shoulder	0, 0, 0	0, 0, 0	0, 1, 0	0, 1, −1	1, 0, 1	0, 1, −1
Left upper arm	0, 0, 0	0, −4, −10	0, 5, −1	−2, 7, −5	−1, −6, 5	−2, 1, −5
Left lower arm	0, 0, 0	−1, −6, −2	−1, −8, −14	−3, −15, −18	−22, −1, −85	0, −30, −34
Left hand	0, 0, 0	0, 0, 1	0, −3, 0	−6, 9, −3	7, −5, 3	−6, 9, −3
Right shoulder	0, 0, 0	−3, −3, 5	1, −3, −1	1, −1, −2	0, −1, 0	1, −1, −2
Right upper arm	0, 0, 0	−1, −6, 12	6, 7, −1	4, 12, −10	1, −5, −13	−2, 13, −1
Right lower arm	0, 0, 0	0, −1, −2	8, 3, 47	8, 4, 44	−1, 9, 2	8, 5, 44
Right hand	0, 0, 0	0, 0, 0	0, 4, −7	0, −2, 2	11, 13, −16	0, −5, −18
Left thigh	0, 0, 0	0, −8, −7	0, −5, −23	−1, 0, −16	2, −8, −2	−1, 0, −17
Left shin	0, 0, 0	0, 0, 1	3, 3, 14	2, 1, 10	4, −1, 44	−3, 10, 38
Left foot	0, 0, 0	−1, 6, 12	−19, −7, −1	−4, −3, 7	3, −6, 13	−4, −3, 7
Right thigh	0, 0, 0	0, 7, 6	−2, 6, 10	7, −1, −35	−1, 9, −51	8, 1, −32
Right shin	0, 0, 0	−1, 1, 10	0, −1, 35	19, 21, 96	−2, 3, 49	10, 24, 108
Right foot	0, 0, 0	−4, −7, −7	−1, −1, −7	7, −16, 18	−5, 2, 16	5, −6, −14

Fig.10, where the upper frames illustrate the changing skeleton sequences, and the bottom frames show the corresponding deformable body surface model. We obtain the animation at about 16.9 frames/second on a PC with Pentium III 733MHz CPU and 256MB memory.

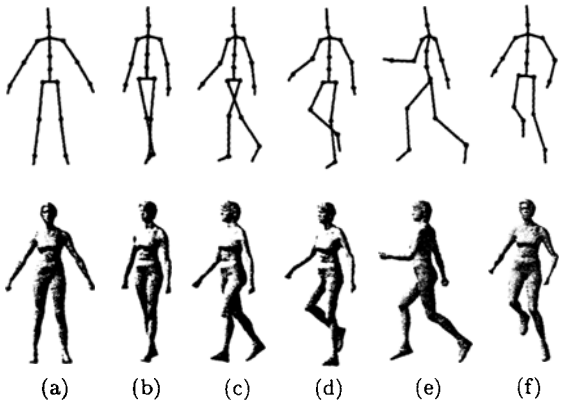

Fig.10. Results of human body animation using motion-captured data.

5 Conclusions and Further Work

We have proposed a framework for modeling the human body from 3D surface scanning data to achieve realistic animation while maintaining sufficient detail. The human model is represented as a layered structure in which the skeleton is built automatically by making use of the detected key landmarks, and the animation is realized by a real-time point-to-line mapping. This procedure is quick and efficient for generating articulated scanned human models without the interaction of the user. The resulting model allows real-time manipulation and rendering, which has sufficient reality for both the shape and the motion posture. It is also possible to rapidly capture and animate new subjects based on existing posture libraries of skeleton models. The model can be used in ergonomic design, garment CAD, real-time simulating humans in virtual reality environment etc.

As some of the assumptions and simplification are used to reduce the complexity of processing, there are several limitations to the current implementation of this approach. The work is still being carried out in order to improve the accuracy. The future work includes the development of a more general algorithm for automatically generating the skeleton of surface model, for example by applying the ideas of segmentation based on detection of branching points to more generic models. Secondly, an efficient deformation algorithm reflecting the muscle deformation should be developed. If we consider the influence of mapped muscle deformation, the results will be more realistic.

Acknowledgements The authors would like to thank Cyberware Inc. for the provision of whole human body data-sets. Thanks also go to Dr. Zhongwei Ying and Dr. Yuping Zhang for helpful suggestions in designing the algorithms.

References

[1] Jones P R M, Rioux M. Three-dimensional surface anthropometry: Applications to the human body. *Optics and Lasers in Engineering*, 1997, 28(2): 89–117.

[2] Hoppe H. Progressive meshes. In *Proc. the ACM SIGGRAPH Conference on Computer Graphics*, ACM Press, 1996, pp.99–108.

[3] Soucy M, Laurendeau D. Multiresolution surface modeling based on hierarchical triangulation. *Computer Vision and Image Understanding*, 1996, 63(1): 1–14.

[4] Liu Y J, Yuen Matthew M F. Optimized triangle mesh reconstruction from unstructured points. *The Visual Computer*, 2003, 19(1): 23–37.

[5] Wang Charlie C L, Chang Terry K K, Yuen Matthew M F. From laser-scanned data to feature human model: A system based on fuzzy logical concept. *Computer-Aided Design*, 2003, 35(3): 241–253.

[6] Lewis J P, Cordner M, Fong N. Pose space deformation: A unified approach to shape interpolation and skeleton-driven deformation. In *Proc. the ACM SIGGRAPH Conference on Computer Graphics*, ACM Press, 2000, pp.165–172.

[7] Shen J, Thalmann D. Interactive shape design using metaballs and splines. In *Proceedings of Eurographics Workshop on Implicit Surfaces'95*, Grenoble, France, 1995, pp.187–196.

[8] Chadwick J E, Haumann, D R, Parent R E. Layered construction for deformable animated characters. *ACM SIGGRAPH Computer Graphics*, 1989, 23(3): 243–252.

[9] Forsey D R. A surface model for skeleton-based character animation. In *Proc. the Second Eurographics Workshop on Animation and Simulation*, Vienna, Austria, 1991, pp.55–73.

[10] Turner R, Gobbetti E. Interactive construction and animation of layered elastically deformable characters. *Computer Graphics Forum*, 1998, 17(2): 135–152.

[11] Lander J. Skin them bones: Game programming for the web generation. *Game Developer Magazine*, 1998, 5: 11–16.

[12] Sun W, Hilton A, Smith R, Illingworth J. Layered animation of captured data. *The Visual Computer*, 2001, 17(8): 457–474.

[13] Brett A, Brian C, Zoran P. Articulated body deformation from range scan data. *ACM Trans. Graphics*, 2002, 21(3): 612–619.

[14] Cyberware Inc. http://www.cyberware.com/.

[15] Dekker L, Khan S, West E, Buxton B, Treleaven P. Models for understanding the 3D human body form. In *Proc. IEEE International Workshop on Model-Based 3D Image Analysis*, Bombay, India, 1998, pp.65–74.

[16] Oliveira J, Buxton B. Light weight virtual humans. In *Proc. Eurographics-UK 2001*, London-UK, 2001, pp.45–52.

[17] Dekker L, Douros I, Buxton B, Treleaven P. Building symbolic information for 3D human body modeling from range data. In *Proc. the Second International Conference on 3D Digital Imaging and Modeling, IEEE Computer Society*, 1999, pp.388–397.

[18] Koivo A J. Fundamentals for Control of Robotics Manipulators, New York, John Wiley & Sons Inc. 1989.

[19] Thomopoulos S C A, Tam R Y J. Interactive solution to the inverse kinematics of robotics manipulators. *Mechanism and Machine Theory*, 1991, 26: 359–373.

[20] Hilton A, Beresford D, Gentils T, Smith R, Wei Sun. Virtual people: Capturing human models to populate virtual worlds. In *IEEE International Conference on Computer Animation Proceedings*, 1999, pp.174–185.

[21] Alvin R T, Henry D A. The Measure of Man and Woman: Human Factors in Design. Revised Edition, New York, John Wiley & Sons Inc. 2001, pp.10–46.

[22] Teichmann M, Teller S. Assisted articulation of closed polygonal models. In *The 9th Eurographics Workshop on Animation and Simulation Proceedings*, 1998, pp.87–101.

[23] Babski C, Thalmann D. A seamless shape for HANIM compliant bodies. In *Proc. VRML 99*, ACM Press, 1999, pp.21–28.

Yong-You Ma received his M.S. degree in mechanical engineering from Kunming University of Science and Technology in 2000. He is currently a Ph.D. candidate in the Institute of Graphical Techniques & CAD, Shanghai Jiaotong University. His research interests include geometric modeling, reverse engineering, computer graphics and animation.

Hui Zhang received his M.S. degree from Gansu University of Technology in 2000. Now he is a Ph.D. candidate in the Institute of Graphical Techniques & CAD, Shanghai Jiaotong University. His main research interests include modern design methodology, visual design, CAD and graphics technology.

Shou-Wei Jiang graduated from Shanghai Jiaotong University in 1960. He is now a professor and Ph.D. supervisor in the School of Mechanical Engineering in Shanghai Jiaotong University. His main research interests include modern design methodology, engineering graphics, CAD and visual design. He has published over 40 papers and 10 books in these fields.